PERGAMON

International Journal of Solids and Structures 38 (2001) 875–895

INTERNATIONAL JOURNAL OF SOLIDS and STRUCTURES

www.elsevier.com/locate/ijsolstr

A damage constitutive model of progressive debonding in aligned discontinuous fiber composites

H.K. Lee *, S. Simunovic

Computer Science and Mathematics Division, Oak Ridge National Laboratory, Oak Ridge, TN 37831-6359, USA

Received 26 July 1999; in revised form 3 March 2000

Abstract

A micromechanical damage constitutive model is presented to predict the overall elastoplastic behavior and damage evolution in aligned discontinuous fiber polymer composites (AFPCs). In an attempt to estimate the overall elastoplastic-damage responses, an effective yield criterion is micromechanically derived based on the ensemble-volume averaging process and first-order (noninteracting) effects of eigenstrains stemming from the existence of (prolate) spheroidal fibers. The proposed effective yield criterion, in conjunction with the assumed overall associative plastic flow rule and hardening law, provides analytical foundation for the estimation of effective elastoplastic behavior of ductile matrix composites. Uniaxial elastoplastic stress–strain behavior of AFPCs is also investigated. An evolutionary interfacial debonding is subsequently employed in accordance with Weibull's probability function to characterize the varying probability of fiber debonding. Finally, the present damage model is compared with Halpin–Tsai's bounds for stiffness predictions and is applied to uniaxial loading to illustrate the damage behavior of AFPCs.

Keywords: Damage constitutive model; Elastoplastic behavior; Progressive debonding; Weibull's probability function

1. Introduction

Damage accumulation in fiber-reinforced organic matrix composites is a complicated progressive phenomenon (Groves et al., 1987; Meraghni and Benzeggagh, 1995; Meraghni et al., 1996). It involves multiple failure modes such as matrix cracking, fiber breakage, delamination, etc., and any of these may begin in an early loading stage and progressively accumulate inside the materials (Wang, 1984; Caslini et al., 1987). The presence of damage can affect the mechanical properties and, subsequently, the response of composites. Accordingly, it is essential in structural application of the composites for the accumulated damage to be predicted and the effect of such damage on the response and failure of the structures to be well determined. Reviews with more details on failure of fiber-reinforced composites can be seen in Matzenmiller and Schweizerhof (1991), Kutlu and Chang (1995), Meraghni and Benzeggagh (1995) and Meraghni et al. (1996).

* Corresponding author. Tel.: +1-423-574-4837; fax: +1-423-574-0680.
E-mail address: leeh@ornl.gov (H.K. Lee).

0020-7683/01/$ - see front matter
PII: S0020-7683(00)00060-3

In general, traditional continuum mechanics is based on the continuity, isotropy and homogeneity of materials. It cannot directly solve the problem for heterogeneous composites since, microscopically, fibers or particles are present within the composites and have a significant effect on the mechanical properties of materials. Hence, micromechanics-based models have been developed to solve the problem on a finer scale and to relate the mechanics of materials to their microstructure. Moreover, micromechanical approaches enable us to evaluate and predict local stress and strain fields in each constituent. The derivation of the constitutive equations in form of a phenomenological parameter model from entirely micromechanical considerations creates a basis of foundation for a rigorous analysis of composite structures.

Although the concept of micromechanics can be traced back to the late 1930s (e.g., Goodier, 1937; Eshelby, 1957, 1959, 1961), micromechanics has been widely developed since 1980s (e.g., Mura, 1987; Nemat-Nasser and Hori, 1993; Mura et al., 1996). Reviews with more details on micromechanical prediction of mechanical properties and failure of composites can be seen by Ju and Chen (1994a) and Krajcinovic (1996), respectively. Most recently, a micromechanical analysis based on the modified Mori–Tanaka method was performed by Meraghni and Benzeggagh (1995) and Meraghni et al. (1996) to address the effect of matrix degradation and interfacial debonding on stiffness reduction in a random discontinuous fiber composite. Their modeling was developed through a methodology of experimental identification of basic damage mechanisms, which involves amplitude analysis of acoustic emission and microscopic observations. Tohgo and Weng (1994) and Zhao and Weng (1995, 1996, 1997) proposed progressive interfacial damage models for ductile matrix composites. They used the probability distribution function of Weibull (1951) to describe the probability of particle debonding. Recently, Ju and Lee (1999) developed a micromechanical damage model to predict the overall elastoplastic behavior and damage evolution in ductile matrix composites. In their derivation, to estimate the overall elastoplastic-damage behavior, an effective yield criterion was derived based on the ensemble-volume averaging procedure and the first-order effects of eigenstrains stemming from the existence of inclusions.

Following the work of Zhao and Weng (1995) and Ju and Lee (1999), we propose a micromechanical damage constitutive model for effective elastoplastic behavior of damaged composite materials to address the damage response of aligned discontinuous fiber polymer composites (AFPCs). In our derivation, fibers are assumed to be elastic (prolate) spheroids which are unidirectionally aligned in a ductile polymer matrix. Furthermore, the ductile matrix behaves *elastoplastically* under arbitrary three-dimensional loading/unloading histories. All fibers are assumed to be *noninteracting* for dilute composite medium and initially embedded firmly in the matrix with perfect interfaces. After the interfacial debonding between fibers and the matrix, these partially debonded fibers are regarded as equivalent, transversely isotropic inclusions. It is worth mentioning that since the scope of this work is to predict the overall damage behavior of AFPCs *globally*, the local microcrack propagation and void nucleation at the interfaces are ignored in our derivation. However, it is possible to extend the proposed damage model to accommodate local damage evolution once new damage growth model and failure criterion are developed based on rigorous experiments. The proposed damage model provides the analytical basis for the estimation of damage behaviors of AFPCs. In the future, the averaging over all orientations upon governing constitutive field equations will be performed to obtain the constitutive relations and the overall yield function for random fiber composites. In addition, a new failure criterion based on experimental verifications for aligned discontinuous fiber-reinforced composites will be also proposed to perform failure analysis of AFPCs.

The present paper is organized as follows: In Section 2, to predict the overall elastoplastic-damage behavior of AFPCs, an "effective yield criterion" is micromechanically constructed based on the ensemble-volume averaging process and the first-order effects of eigenstrains due to the existence of aligned discontinuous fibers. The proposed elastoplastic-damage formulation is applied to uniaxial loading condition in Section 2. An evolutionary interfacial debonding model is considered in accordance with Weibull's statistical function to address the varying probability of fiber debonding in Section 3. The explicit relationship is also derived in Section 3 to relate the average internal stresses of fibers and the macroscopic total

strain. In Section 4, the present damage model is compared with theoretical bounds and is applied to the uniaxial tensile loading to predict the various stress–strain responses of AFPCs.

2. Overall elastoplastic behavior of ACFPMCs: a micromechanical framework

2.1. Effective elastic moduli of composites with aligned discontinuous fibers

Let us start by considering an initially perfectly bonded two-phase composite consisting of a matrix (phase 0) with bulk modulus κ_0 and shear modulus μ_0, and aligned discontinuous, randomly dispersed (prolate) spheroidal fibers (phase 1) with bulk modulus κ_1 and shear modulus μ_1. When spheroidal inclusions (discontinuous fibers) are aligned in the 1-direction, the composite as a whole is transversely isotropic. Subsequently, as loadings or deformations are applied, some fibers are partially debonded (phase 2), and these partially debonded fibers are regarded as equivalent, transversely isotropic inclusions.

Following Zhao and Weng (1996, 1997), a partially debonded fiber can be replaced by an equivalent, perfectly bonded fiber which possesses yet unknown transversely isotropic moduli. The transverse isotropy of the equivalent fiber can be determined in such a way that (a) its tensile and shear stresses will always vanish in the debonded direction, and (b) its stresses in the bonded directions exist, since the fiber is still able to transmit stresses to the matrix on the bonded surfaces.

When the 1-direction is chosen as symmetric and the plane 2–3 isotropic, the stress–strain relation of a typical transversely isotropic solid can be written as

$$\begin{pmatrix} \sigma_{11} \\ \sigma_{22} \\ \sigma_{33} \\ \sigma_{23} \\ \sigma_{13} \\ \sigma_{12} \end{pmatrix} = \begin{bmatrix} C_{11} & C_{12} & C_{12} & 0 & 0 & 0 \\ C_{12} & C_{22} & C_{23} & 0 & 0 & 0 \\ C_{12} & C_{23} & C_{22} & 0 & 0 & 0 \\ 0 & 0 & 0 & C_{44} & 0 & 0 \\ 0 & 0 & 0 & 0 & C_{55} & 0 \\ 0 & 0 & 0 & 0 & 0 & C_{55} \end{bmatrix} \begin{pmatrix} \epsilon_{11} \\ \epsilon_{22} \\ \epsilon_{33} \\ 2\epsilon_{23} \\ 2\epsilon_{13} \\ 2\epsilon_{12} \end{pmatrix}. \tag{1}$$

The components of the stiffness matrix take the form

$$\begin{aligned} &\tfrac{C_{22}+C_{23}}{2} = k, \qquad C_{12} = l, \qquad C_{11} = \bar{n}, \\ &\tfrac{C_{22}-C_{23}}{2} = C_{44} = m, \qquad C_{55} = p, \end{aligned} \tag{2}$$

where k is the plane stress bulk modulus for the lateral dilatation without longitudinal extension ($k = \kappa + \mu/3$), m is the rigidity modulus for shearing in any transverse direction, $\bar{n}$ denotes the modulus for the longitudinal uniaxial straining, l denotes the associated cross-modulus and p signifies the axial shear modulus (Hill, 1964). Therefore, the stress–strain relations for partially debonded composite can be rephrased as

$$\begin{aligned} &\tfrac{1}{2}(\sigma_{22} + \sigma_{33}) = k(\epsilon_{22} + \epsilon_{33}) + l\epsilon_{11}, \\ &\sigma_{11} = l(\epsilon_{22} + \epsilon_{33}) + \bar{n}\epsilon_{11}, \\ &\sigma_{22} - \sigma_{33} = 2m(\epsilon_{22} - \epsilon_{33}), \\ &\sigma_{23} = 2m\epsilon_{23}, \qquad \sigma_{12} = 2p\epsilon_{12}, \qquad \sigma_{13} = 2p\epsilon_{13}. \end{aligned} \tag{3}$$

It can be easily seen that, by using the inverse of generalized Hook's law, the compliance matrix for a transversely isotropic material may be expressed in the form

$$\begin{pmatrix} \epsilon_{11} \\ \epsilon_{22} \\ \epsilon_{33} \\ 2\epsilon_{23} \\ 2\epsilon_{13} \\ 2\epsilon_{12} \end{pmatrix} = \begin{bmatrix} \frac{k}{l^2+k\bar{n}} & \frac{l}{2(l^2-k\bar{n})} & \frac{l}{2(l^2-k\bar{n})} & 0 & 0 & 0 \\ \frac{l}{2(l^2-k\bar{n})} & \frac{-l^2+k\bar{n}+m\bar{n}}{4m(-l^2+k\bar{n})} & \frac{l^2-k\bar{n}+m\bar{n}}{4m(-l^2+k\bar{n})} & 0 & 0 & 0 \\ \frac{l}{2(l^2-k\bar{n})} & \frac{l^2-k\bar{n}+m\bar{n}}{4m(-l^2+k\bar{n})} & \frac{-l^2+k\bar{n}+m\bar{n}}{4m(-l^2+k\bar{n})} & 0 & 0 & 0 \\ 0 & 0 & 0 & \frac{1}{m} & 0 & 0 \\ 0 & 0 & 0 & 0 & \frac{1}{p} & 0 \\ 0 & 0 & 0 & 0 & 0 & \frac{1}{p} \end{bmatrix} \begin{pmatrix} \sigma_{11} \\ \sigma_{22} \\ \sigma_{33} \\ \sigma_{23} \\ \sigma_{13} \\ \sigma_{12} \end{pmatrix}. \tag{4}$$

For the special case of uniaxial loading, Eq. (4) can be simplified as

$$\epsilon_{ij} = \begin{bmatrix} \frac{k}{-l^2+k\bar{n}} & 0 & 0 \\ 0 & \frac{l}{2(l^2-k\bar{n})} & 0 \\ 0 & 0 & \frac{l}{2(l^2-k\bar{n})} \end{bmatrix} \sigma_{11}. \tag{5}$$

The transversely isotropic fiber can be considered to be under the condition of plane stress with the components in the 1-direction being zero. To ensure the equivalence between a partially debonded isotropic fiber and an equivalent, perfectly bonded transversely isotropic fiber, the elastic moduli of a transversely isotropic fiber, with the condition $\sigma_{11} = \sigma_{12} = \sigma_{13} = 0$, can be derived as

$$k_2 = \frac{\mu_1(3k_1 - \mu_1)}{k_1 + \mu_1}, \qquad l_2 = 0, \quad \bar{n}_2 = 0, \quad m_2 = \mu_1, \quad p_2 = 0, \tag{6}$$

where the subscripts 1 and 2 refer to phases 1 and 2 moduli, respectively.

In accordance with the notation given in Eq. (2), the stiffness tensor $\mathbf{C}_2$ for the equivalent, transversely isotropic fiber can be represented as

$$\mathbf{C}_2 = \tilde{F}_{ijkl}(t_1, t_2, t_3, t_4, t_5, t_6), \tag{7}$$

where a transversely isotropic fourth-rank tensor $\tilde{\mathbf{F}}$ is defined by six parameters b_m ($m = 1$–6):

$$\begin{aligned} \tilde{F}_{ijkl}(b_m) = {} & b_1\tilde{n}_i\tilde{n}_j\tilde{n}_k\tilde{n}_l + b_2(\delta_{ik}\tilde{n}_j\tilde{n}_l + \delta_{il}\tilde{n}_j\tilde{n}_k + \delta_{jk}\tilde{n}_i\tilde{n}_l + \delta_{jl}\tilde{n}_i\tilde{n}_k) \\ & + b_3\delta_{ij}\tilde{n}_k\tilde{n}_l + b_4\delta_{kl}\tilde{n}_i\tilde{n}_j + b_5\delta_{ij}\delta_{kl} + b_6(\delta_{ik}\delta_{jl} + \delta_{il}\delta_{jk}), \end{aligned} \tag{8}$$

where $\tilde{n}$ denotes the unit vector and δ_{ij} signifies the Kronecker delta. For a spheroid of $a_1 \neq a_2 = a_3$, the 1-direction is chosen as symmetric and therefore we have $\tilde{n}_1 = 1,\ \tilde{n}_2 = \tilde{n}_3 = 0$. In addition, the six parameters on the right-hand side of Eq. (7) take the form

$$t_1 = k_2 + \bar{n}_2 + m_2 - 4p_2 - 2l_2, \tag{9}$$

$$t_2 = -m_2 + p_2, \tag{10}$$

$$t_3 = -k_2 + m_2 + l_2, \tag{11}$$

$$t_4 = -k_2 + m_2 + l_2, \tag{12}$$

$$t_5 = k_2 - m_2, \tag{13}$$

$$t_6 = m_2. \tag{14}$$

When considering the strain and stress fields at a local point $\mathbf{x}$ that is outside an inclusion, we define a fourth-rank tensor $\bar{\mathbf{G}}(\mathbf{x})$, which is called the *exterior-point Eshelby's tensor* as (see, Eshelby, 1959; Mura, 1987)

$$\bar{\mathbf{G}}(\mathbf{x}) \equiv \int_{\Omega} \mathbf{G}(\mathbf{x} - \mathbf{x}')\,\mathrm{d}\mathbf{x}' \quad (\mathbf{x} \in V - \Omega), \tag{15}$$

where V is the volume of a representative volume element and Ω denotes the inclusion domain.

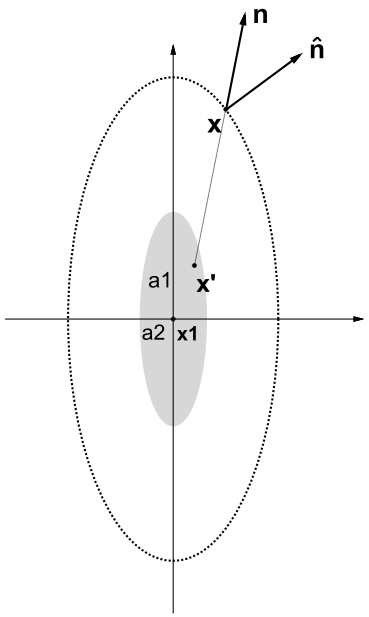

Fig. 1. Schematic description of an imaginary ellipsoid surface and its unit outward normal vector.

Exterior-point Eshelby's tensor $\bar{\mathbf{G}}(\mathbf{x})$ of an ellipsoidal inclusion can be derived by introducing an unit outward normal vector $\hat{\mathbf{n}}$, shown in Fig. 1, at a matrix point $\mathbf{x}$ on the new imaginary ellipsoid surface which can be defined as (see also Sun, 1998)

$$\hat{n}_i = \frac{x_i}{(a_i^2 + \vartheta)\sqrt{\Theta(\vartheta)}}, \tag{16}$$

where

$$\Theta(\vartheta) \equiv \Theta_i(\vartheta)\Theta_i(\vartheta), \tag{17}$$

$$\Theta_i(\vartheta) \equiv \frac{x_i}{a_i^2 + \vartheta} \tag{18}$$

in which a_i $(i = 1, 2, 3)$ is one of the three semi-axes of the ellipsoid and ϑ is taken as positive and can be uniquely solved in terms of local point $\mathbf{x}$ of matrix and a_i. Ju and Sun (1998) explicitly derived the exterior-point Eshelby's tensor $\bar{\mathbf{G}}(\mathbf{x})$ of an ellipsoidal inclusion.

As a special case of an ellipsoid, if two of the three semi-axes of the ellipsoid are the same, then the ellipsoid will become a spheroid. Let us assume that $a_1 \neq a_2 = a_3$, where the spheroid aspect ratio α is defined as $\alpha \equiv a_1/a_2$. (Interior-point) Eshelby's tensor of a spheroidal inclusion can be obtained in a transversely isotropic fourth-rank tensor form by letting $\lambda = 0$ in the exterior-point Eshelby's tensor given by Ju and Sun (1998) as

$$\begin{aligned}\mathbf{S}(\mathbf{x}) &\equiv \int_{\Omega} \mathbf{G}(\mathbf{x} - \mathbf{x}')\mathrm{d}\mathbf{x}', \quad \mathbf{x} \in \Omega \\ &= \tilde{F}_{ijkl}(S_1, S_2, S_3, S_4, S_5, S_6),\end{aligned} \tag{19}$$

where the six parameters on the right-hand side of Eq. (19) take the form

$$S_1 = \frac{1}{16}\frac{16 + 45\varpi + 54\alpha^2 + 60\varpi\alpha^2}{(\nu_0 - 1)(1 - \alpha^2)}, \tag{20}$$

$$S_2 = \frac{1}{16}\frac{8 + 15\varpi - 8\nu_0 - 12\varpi\nu_0 + 2\alpha^2 + 8\nu_0\alpha^2 + 12\varpi\nu_0\alpha^2}{1 - \nu_0 - \alpha^2 + \nu_0\alpha^2}, \tag{21}$$

$$S_3 = \frac{1}{16}\frac{3\varpi + 10\alpha^2 + 12\varpi\alpha^2}{(\nu_0 - 1)(\alpha^2 - 1)}, \tag{22}$$

$$S_4 = \frac{1}{16}\frac{3\varpi + 16\nu_0 + 24\varpi\nu_0 + 10\alpha^2 + 12\varpi\alpha^2 - 16\nu_0\alpha^2 - 24\nu_0\varpi\alpha^2}{(\nu_0 - 1)(\alpha^2 - 1)}, \tag{23}$$

$$S_5 = \frac{1}{16}\frac{\varpi - 8\varpi\nu_0 - 2\alpha^2 - 4\varpi\alpha^2 + 8\nu_0\varpi\alpha^2}{(\nu_1 - 1)(\alpha^2 - 1)}, \tag{24}$$

$$S_6 = \frac{1}{16}\frac{-7\varpi + 8\nu_0\varpi - 2\alpha^2 + 4\varpi\alpha^2 - 8\nu_0\varpi\alpha^2}{1 - \nu_0 - \alpha^2 + \nu_0\alpha^2} \tag{25}$$

with

$$\varpi = \begin{cases} \frac{\alpha}{(\alpha^2-1)^{3/2}}\left[\cosh^{-1}\alpha - \alpha(\alpha^2 - 1)^{1/2}\right] & \text{for } \alpha > 1, \\ \frac{\alpha}{(1-\alpha^2)^{3/2}}\left[\alpha(1 - \alpha^2)^{1/2} - \cos^{-1}\alpha\right] & \text{for } \alpha < 1. \end{cases} \tag{26}$$

It is noted that Eshelby's tensor for a spheroidal inclusion in Eqs. (20)–(25) should be identical to the results of Ju and Sun (1998).

Effective elastic moduli of multi-phase composites containing randomly located, unidirectionally aligned elastic ellipsoids were explicitly derived by Ju and Chen (1994a) accounting for far-field perturbations. For a multi-phase composite, the effective elasticity tensor $\mathbf{C}_*$ assuming no interaction among constituents reads

$$\mathbf{C}_* = \mathbf{C}_0 \cdot \left\{\mathbf{I} + \mathbf{B} \cdot (\mathbf{I} - \mathbf{S} \cdot \mathbf{B})^{-1}\right\}, \tag{27}$$

where $\mathbf{I}$ is the fourth-rank identity tensor, "$\cdot$" denotes the tensor multiplication and $\mathbf{B}$ takes the form,

$$\mathbf{B} = \sum_{q=1}^{n} \phi_q (\mathbf{S} + \mathbf{A}_q)^{-1}, \tag{28}$$

in which n signifies the number of inclusion phases of different material properties, and ϕ_q denotes the volume fraction of the q-phase. In addition, the fourth-rank tensor $\mathbf{A}_q$ is defined as

$$\mathbf{A}_q = [\mathbf{C}_q - \mathbf{C}_0]^{-1} \cdot \mathbf{C}_0. \tag{29}$$

Accordingly, in the case of aligned (in the x_1-direction) fiber-reinforced composites, the effective elastic stiffness tensor $\mathbf{C}_*$ can be explicitly derived as

$$\mathbf{C}_* = \tilde{F}_{ijkl}(\iota_1, \iota_2, \iota_3, \iota_4, \iota_5, \iota_6), \tag{30}$$

where the parameters of $\iota_1, \ldots, \iota_6$ are

$$\begin{aligned} \iota_1 &= \psi_{11} - \psi_{12} - \psi_{21} + \psi_{22} + 2\varphi_1 + 2\varphi_2 - 4\varphi_3, \\ \iota_2 &= -\varphi_2 + \varphi_3, \\ \iota_3 &= \psi_{21} - \psi_{22}, \\ \iota_4 &= \psi_{12} - \psi_{22}, \\ \iota_5 &= \psi_{22}, \\ \iota_6 &= \varphi_2 \end{aligned} \tag{31}$$

in which the parameters $\psi_{11},\ldots,\psi_{22}$ and $\varphi_1,\ldots,\varphi_3$ are given in Appendix A. In addition, the five effective elastic moduli of composites with aligned discontinuous fibers read

$$k_* = \iota_5 + \iota_6, \qquad l_* = \iota_4 + \iota_5, \qquad m_* = \iota_6,$$
$$\bar{n}_* = \iota_1 + 4\iota_2 + \iota_3 + \iota_4 + \iota_5 + 2\iota_6, \qquad p_* = \iota_2 + \iota_6. \tag{32}$$

2.2. Effective elastoplastic behavior of composites with aligned discontinuous fibers

We now consider the overall elastoplastic responses of progressively debonded fiber-reinforced composites which initially feature perfect interfacial bonding between fibers and the matrix in two-phase composites. It is known that partial interfacial debonding may occur in some fibers under applied loading. Therefore, an original two-phase composite may gradually become a three-phase composite consisting of the matrix, perfectly bonded fibers and partially debonded fibers. In what follows, for simplicity, we will regard partially debonded fibers as equivalent, perfectly bonded transversely isotropic fibers. For simplicity, the von Mises yield criterion with isotropic hardening law is assumed here. Accordingly, at any matrix material point, the stress $\boldsymbol{\sigma}$ and the equivalent plastic strain $\bar{e}^{\mathrm{p}}$ must satisfy the following yield function:

$$F(\boldsymbol{\sigma}, \bar{e}^{\mathrm{p}}) = H(\boldsymbol{\sigma}) - K^2(\bar{e}^{\mathrm{p}}) \leqslant 0, \tag{33}$$

in which $K(\bar{e}^{\mathrm{p}})$ is the isotropic hardening function of the matrix-only material. Furthermore, $H(\boldsymbol{\sigma}) \equiv \boldsymbol{\sigma} : \mathbf{I}_{\mathrm{d}} : \boldsymbol{\sigma}$ denotes the square of the deviatoric stress norm, where $\mathbf{I}_{\mathrm{d}}$ signifies the *deviatoric* part of the fourth-rank identity tensor $\mathbf{I}$, i.e.,

$$\mathbf{I}_{\mathrm{d}} \equiv \mathbf{I} - \tfrac{1}{3}\mathbf{1} \otimes \mathbf{1}, \tag{34}$$

in which $\mathbf{1}$ represents the second-rank identity tensor and "$\otimes$" denotes the tensor expansion.

Following Ju and Lee (1999), we denote by $H(\mathbf{x}|\mathscr{G})$ the square of the "current stress norm" at the local point $\mathbf{x}$, which determines the plastic strain in a composite for a given phase configuration $\mathscr{G}$. Since there is no plastic strain in the elastic perfectly bonded fibers or partially debonded fibers, $H(\mathbf{x}|\mathscr{G})$ can be written as

$$H(\mathbf{x}|\mathscr{G}) = \begin{cases} \boldsymbol{\sigma}(\mathbf{x}|\mathscr{G}) : \mathbf{I}_{\mathrm{d}} : \boldsymbol{\sigma}(\mathbf{x}|\mathscr{G}) & \text{if } \mathbf{x} \text{ in the matrix,} \\ 0, & \text{otherwise.} \end{cases} \tag{35}$$

In addition, $\langle H \rangle_m(\mathbf{x})$ is defined as the ensemble average of $H(\mathbf{x}|\mathscr{G})$ over all possible realizations where $\mathbf{x}$ is in the matrix phase. Here, the angled bracket $\langle\cdot\rangle$ signifies the ensemble average operator. Let $P(\mathscr{G}_q)$ be the probability density function for finding the q-phase ($q = 1, 2$) configuration $\mathscr{G}_q$ in the composite. $\langle H \rangle_m(\mathbf{x})$ can be obtained by integrating H over all possible perfectly bonded fibers and partially debonded fibers configurations (for a point $\mathbf{x}$ in the matrix)

$$\langle H \rangle_m(\mathbf{x}) = H^0 + \int_{\mathscr{G}_1} \{H(\mathbf{x}|\mathscr{G}_1) - H^0\} P(\mathscr{G}_1)\, \mathrm{d}\mathscr{G} + \int_{\mathscr{G}_2} \{H(\mathbf{x}|\mathscr{G}_2) - H^0\} P(\mathscr{G}_2)\, \mathrm{d}\mathscr{G}, \tag{36}$$

where H^0 is the square of the far-field stress norm in the matrix:

$$H^0 = \boldsymbol{\sigma}^0 : \mathbf{I}_{\mathrm{d}} : \boldsymbol{\sigma}^0. \tag{37}$$

As indicated, a matrix point receives the perturbations from perfectly bonded fibers and partially debonded fibers. Therefore, the ensemble-average stress norm for any matrix point $\mathbf{x}$ can be evaluated by collecting and summing up all the current stress norm perturbations produced by any typical perfectly bonded fiber centered at $\mathbf{x}_1^{(1)}$ in the perfectly bonded fiber domain and any typical partially debonded fiber centered at $\mathbf{x}_2^{(1)}$ in the partially debonded fiber domain, and averaging over all possible locations of $\mathbf{x}_1^{(1)}$ and $\mathbf{x}_2^{(1)}$. As a result, we arrive at

$$\langle H\rangle_m(\mathbf{x}) \cong H^0 + \int_{\mathbf{x}_1^{(1)}\notin\Xi(\mathbf{x})} \left\{H\left(\mathbf{x}|\mathbf{x}_1^{(1)}\right) - H^0\right\} P\left(\mathbf{x}_1^{(1)}\right)\, \mathrm{d}\mathbf{x}_1^{(1)} + \int_{\mathbf{x}_2^{(1)}\notin\Xi(\mathbf{x})} \left\{H\left(\mathbf{x}|\mathbf{x}_2^{(1)}\right) - H^0\right\} \times P\left(\mathbf{x}_2^{(1)}\right)\, \mathrm{d}\mathbf{x}_2^{(1)} + \cdots, \tag{38}$$

where $\Xi(\mathbf{x})$ is the exclusion zone and $P(\mathbf{x}_1^{(1)})$ and $P(\mathbf{x}_2^{(1)})$ denote the probability density functions for finding a perfectly bonded fiber centered at $\mathbf{x}_1^{(1)}$ and a partially debonded fiber centered at $\mathbf{x}_2^{(1)}$, respectively. Here, for simplicity, $P(\mathbf{x}_1^{(1)})$ and $P(\mathbf{x}_2^{(1)})$ are assumed to be statistically homogeneous, isotropic and uniform. That is, we assume that the probability density functions take the form $P(\mathbf{x}_1^{(1)}) = N_1/V$ and $P(\mathbf{x}_2^{(1)}) = N_2/V$, where N_1 and N_2 are the total numbers of perfectly bonded fibers and partially debonded fibers, respectively, dispersed in a representative volume V. We define a tiny equal-volume spherical probabilistic zone with the radius $a^* = (a_1 a_2^2)^{1/3}$, or $a^* = a_1/\alpha^{2/3}$, where $\alpha = a_1/a_2$ is the aspect ratio (the ratio of length to diameter) of a spheroid. Further, owing to the assumption of statistical isotropy and uniformity, Eq. (38) can be recast into a more convenient form:

$$\langle H\rangle_m(\mathbf{x}) \cong H^0 + \frac{N_1}{V}\int_{\hat{r}_1>a^*} \mathrm{d}\hat{r}_1 \int_{A(\hat{r}_1)} \{H(\hat{\mathbf{r}}_1) - H^0\}\, \mathrm{d}A + \frac{N_2}{V}\int_{\hat{r}_2>a^*} \mathrm{d}\hat{r}_2 \int_{A(\hat{r}_2)} \{H(\hat{\mathbf{r}}_2) - H^0\}\, \mathrm{d}A + \cdots, \tag{39}$$

where $A(\hat{r}_q)$ is a spherical surface of radius $\hat{r}_q$ $(q = 1, 2)$ in the probability space.

By dropping the higher order terms, the integral on the right-hand side of Eq. (39) can be evaluated and we arrive at the ensemble-averaged current stress norm at any matrix point

$$\langle H\rangle_m(\mathbf{x}) = \boldsymbol{\sigma}^0 : \mathbf{T} : \boldsymbol{\sigma}^0. \tag{40}$$

The components of the positive definite fourth-rank tensor $\mathbf{T}$ read

$$T_{ijkl} = \tilde{F}_{ijkl}(\bar{t}_1, \bar{t}_2, \bar{t}_3, \bar{t}_4, \bar{t}_5, \bar{t}_6), \tag{41}$$

where the six parameters on the right-hand side take the form,

$$\begin{aligned}
\bar{t}_1 &= \mathscr{M}_{11} - \mathscr{M}_{12} - \mathscr{M}_{21} + \mathscr{M}_{22} + 2\mathscr{N}_1 + 2\mathscr{N}_2 - 4\mathscr{N}_3,\\
\bar{t}_2 &= -\mathscr{N}_2 + \mathscr{N}_3,\\
\bar{t}_3 &= \mathscr{M}_{21} - \mathscr{M}_{23},\\
\bar{t}_4 &= \mathscr{M}_{12} - \mathscr{M}_{23},\\
\bar{t}_5 &= \mathscr{M}_{23},\\
\bar{t}_6 &= \mathscr{N}_2,
\end{aligned} \tag{42}$$

in which the parameters $\mathscr{M}_{ij}$ and $\mathscr{N}_i$ are given in Appendix B.

The ensemble-averaged current stress norm at a matrix point can also be expressed in terms of the macroscopic stress $\bar{\boldsymbol{\sigma}}$. Following Ju and Chen (1994a), the relation between the far-field stress $\boldsymbol{\sigma}^0$ and the macroscopic stress $\bar{\boldsymbol{\sigma}}$ takes the form

$$\boldsymbol{\sigma}^0 = \mathbf{P} : \bar{\boldsymbol{\sigma}}, \tag{43}$$

where the fourth-rank tensor $\mathbf{P}$ reads

$$\mathbf{P} = \mathbf{I} + \sum_{r=1}^{2} \phi_r (\mathbf{I} - \mathbf{S}) \cdot (\mathbf{A}_r + \mathbf{S})^{-1} = \tilde{F}_{ijkl}(p_1, p_2, p_3, p_4, p_5, p_6) \tag{44}$$

and the components $p_1, \ldots, p_6$ are

$$p_1 = \mathscr{H}_{11} - \mathscr{H}_{12} - \mathscr{H}_{21} + \mathscr{H}_{22} + 2\mathscr{I}_1 + 2\mathscr{I}_2 - 4\mathscr{I}_3, \tag{45}$$

$$p_2 = -\mathscr{I}_2 + \mathscr{I}_3, \tag{46}$$

$$p_3 = \mathscr{H}_{21} - \mathscr{H}_{23}, \tag{47}$$

$$p_4 = \mathscr{H}_{12} - \mathscr{H}_{23}, \tag{48}$$

$$p_5 = \mathscr{H}_{23}, \tag{49}$$

$$p_6 = \mathscr{I}_2 \tag{50}$$

with

$$\mathscr{H}_{ij} = -\frac{\mathscr{J}_{ij}}{2\mathscr{K}_i} \quad (i,j = 1,2,3), \tag{51}$$

$$\mathscr{I}_i = \frac{1}{4\mathscr{K}_i} \quad (i = 1,2,3), \tag{52}$$

where

$$\mathscr{J}_{i1} = \frac{(\mathscr{L}_{22} + \mathscr{K}_2)\mathscr{L}_{i1} - \mathscr{L}_{21}\mathscr{L}_{i2}}{(\mathscr{L}_{11} + 2\mathscr{K}_1)(\mathscr{L}_{22} + \mathscr{K}_2) - \mathscr{L}_{12}\mathscr{L}_{21}} \quad (i = 1,2,3), \tag{53}$$

$$\mathscr{J}_{i2} = \mathscr{J}_{i3} = \frac{(\mathscr{L}_{11} + 2\mathscr{K}_1)\mathscr{L}_{i2} - \mathscr{L}_{12}\mathscr{L}_{i1}}{2(\mathscr{L}_{11} + 2\mathscr{K}_1)(\mathscr{L}_{22} + \mathscr{K}_2) - 2\mathscr{L}_{12}\mathscr{L}_{21}} \quad (i = 1,2,3), \tag{54}$$

$$\mathscr{K}_i = \frac{1}{2} + \sum_{r=1}^{2} \frac{(1 - 2\mathscr{B}_i)\phi_r}{2(\mathscr{V}_r)_i} \quad (i = 1,2,3), \tag{55}$$

$$\mathscr{L}_{ij} = \sum_{r=1}^{2} \phi_r \left[\sum_{n=1}^{3} \frac{(\mathscr{W}_r)_{nj}\bar{\mathscr{A}}_{in}}{(\mathscr{V}_r)_n} - \frac{\bar{\mathscr{A}}_{ij}}{(\mathscr{V}_r)_j} - \frac{(\mathscr{W}_r)_{ij}(1 - 2\bar{\mathscr{B}}_{ii})}{(\mathscr{V}_r)_i} \right] \quad (i,j = 1,2,3). \tag{56}$$

By combining Eqs. (40) and (43), we arrive at the alternative expression for the ensemble-averaged current stress norm (square) in a matrix point

$$\langle H \rangle_m(\mathbf{x}) = \bar{\boldsymbol{\sigma}} : \bar{\mathbf{T}} : \bar{\boldsymbol{\sigma}}, \tag{57}$$

where the positive definite fourth-rank tensor $\bar{\mathbf{T}}$ is defined as

$$\bar{\mathbf{T}} \equiv \mathbf{P}^{\mathrm{T}} \cdot \mathbf{T} \cdot \mathbf{P} \tag{58}$$

and can be shown to be

$$\begin{aligned} \bar{T}_{ijkl} = {} & \bar{T}_1 \tilde{n}_i \tilde{n}_j \tilde{n}_k \tilde{n}_l + \bar{T}_2(\delta_{ik}\tilde{n}_j\tilde{n}_l + \delta_{il}\tilde{n}_j\tilde{n}_k + \delta_{jk}\tilde{n}_i\tilde{n}_l + \delta_{jl}\tilde{n}_i\tilde{n}_k) \\ & + \bar{T}_3\delta_{ij}\tilde{n}_k\tilde{n}_l + \bar{T}_4\delta_{kl}\tilde{n}_i\tilde{n}_j + \bar{T}_5\delta_{ij}\delta_{kl} + \bar{T}_6(\delta_{ik}\delta_{jl} + \delta_{il}\delta_{jk}), \end{aligned} \tag{59}$$

where the components $\bar{T}_1, \ldots, \bar{T}_6$ are given in Appendix C.

The ensemble-volume averaged "current stress norm" for any point $\mathbf{x}$ in AFPCs can be defined as

$$\sqrt{\langle H \rangle(\mathbf{x})} = (1 - \phi_1)\sqrt{\bar{\boldsymbol{\sigma}} : \bar{\mathbf{T}} : \bar{\boldsymbol{\sigma}}}, \tag{60}$$

where ϕ_1 is the current volume fraction of perfectly bonded fibers. Therefore, the effective yield function for the three-phase AFPCs can be proposed as

$$\bar{F} = (1 - \phi_1)^2 \bar{\boldsymbol{\sigma}} : \bar{\mathbf{T}} : \bar{\boldsymbol{\sigma}} - K^2(\bar{e}^{\mathrm{p}}) \tag{61}$$

with the isotropic hardening function $K(\bar{e}^{\mathrm{p}})$ for the three-phase composite. The effective ensemble-volume averaged plastic strain rate for the AFPCs can be expressed as

$$\dot{\bar{\boldsymbol{\epsilon}}}^{\mathrm{p}} = \dot{\lambda}\frac{\partial \bar{F}}{\partial \bar{\boldsymbol{\sigma}}} = 2(1-\phi_1)^2\dot{\lambda}\bar{\mathbf{T}} : \bar{\boldsymbol{\sigma}}, \tag{62}$$

where $\dot{\lambda}$ denotes the plastic consistency parameter.

Inspired by the structure of the micromechanically derived stress norm, the effective equivalent plastic strain rate for the composite is defined as

$$\dot{\bar{e}}^{\mathrm{p}} \equiv \sqrt{\tfrac{2}{3}\dot{\bar{\boldsymbol{\epsilon}}}^{\mathrm{p}} : \bar{\mathbf{T}}^{-1} : \dot{\bar{\boldsymbol{\epsilon}}}^{\mathrm{p}}} = 2(1-\phi_1)^2\dot{\lambda}\sqrt{\tfrac{2}{3}\bar{\boldsymbol{\sigma}} : \bar{\mathbf{T}} : \bar{\boldsymbol{\sigma}}}. \tag{63}$$

The $\dot{\lambda}$ together with the yield function $\bar{F}$ must obey the *Kuhn–Tucker* loading/unloading conditions. In what follows, the simple power-law type isotropic hardening function is employed as an example

$$K(\bar{e}^{\mathrm{p}}) = \sqrt{\tfrac{2}{3}}\left\{\sigma_{\mathrm{y}} + h(\bar{e}^{\mathrm{p}})^{\bar{q}}\right\}, \tag{64}$$

where σ_{y} is the initial yield stress, and h and $\bar{q}$ signify the linear and exponential isotropic hardening parameters, respectively, for the three-phase composite.

2.3. Elastoplastic stress–strain relationship for partially debonded three-phase AFPCs

In order to illustrate the proposed micromechanics-based elastoplastic constitutive damage model for AFPCs, let us consider the example of *uniaxial* tensile loading.

The applied macroscopic stress $\bar{\sigma}$ can be written as

$$\bar{\sigma}_{11} \neq 0, \quad \text{all other } \bar{\sigma}_{ij} = 0. \tag{65}$$

With the simple isotropic hardening law described by Eq. (64), the overall yield function reads

$$\bar{F}(\bar{\boldsymbol{\sigma}}, \bar{e}^{\mathrm{p}}) = (1-\phi_1)^2\bar{\boldsymbol{\sigma}} : \bar{\mathbf{T}} : \bar{\boldsymbol{\sigma}} - \tfrac{2}{3}\left\{\sigma_{\mathrm{y}} + h(\bar{e}^{\mathrm{p}})^{\bar{q}}\right\}^2. \tag{66}$$

Substituting Eq. (65) into Eq. (66), the effective yield function of partially debonded three-phase AFPCs for uniaxial loading is obtained as

$$\bar{F} = (1-\phi_1)^2(\bar{T}_1 + 4\bar{T}_2 + \bar{T}_3 + \bar{T}_4 + \bar{T}_5 + 2\bar{T}_6)\bar{\sigma}_{11}^2 - \tfrac{2}{3}\left\{\sigma_{\mathrm{y}} + h(\bar{e}^{\mathrm{p}})^{\bar{q}}\right\}^2. \tag{67}$$

The macroscopic incremental plastic strain rate defined by Eq. (62) becomes

$$\Delta\bar{\boldsymbol{\epsilon}}^{\mathrm{p}} = 2(1-\phi_1)^2\Delta\lambda\,\bar{\sigma}_{11}\begin{pmatrix} \bar{T}_1 + 4\bar{T}_2 + \bar{T}_3 + \bar{T}_4 + \bar{T}_5 + 2\bar{T}_6 & 0 & 0 \\ 0 & \bar{T}_3 + \bar{T}_5 & 0 \\ 0 & 0 & \bar{T}_3 + \bar{T}_5 \end{pmatrix} \tag{68}$$

for any stress beyond the initial yielding. Similarly, the incremental equivalent plastic strain can be written as

$$\Delta\bar{\mathrm{e}}^{\mathrm{p}} = 2(1-\phi_1)^2\Delta\lambda|\bar{\sigma}_{11}|\sqrt{\tfrac{2}{3}(\bar{T}_1 + 4\bar{T}_2 + \bar{T}_3 + \bar{T}_4 + \bar{T}_5 + 2\bar{T}_6)}. \tag{69}$$

From Eqs. (5) and (32), the macroscopic incremental elastic strain takes the form

$$\Delta\bar{\boldsymbol{\epsilon}}^{\mathrm{e}} = \begin{bmatrix} \frac{k_*}{-l_*^2 + k_*\bar{n}_*} & 0 & 0 \\ 0 & \frac{l_*}{2(l_*^2 - k_*\bar{n}_*)} & 0 \\ 0 & 0 & \frac{l_*}{2(l_*^2 - k_*\bar{n}_*)} \end{bmatrix}\Delta\bar{\sigma}_{11}. \tag{70}$$

Furthermore, the total incremental strain is the sum of the elastic incremental strain and plastic incremental strain.

The positive parameter $\lambda = \sum_i (\Delta\lambda)^i$ is solved from the nonlinear equation obtained by enforcing the plastic consistency condition $\bar{F} = 0$. Since only the uniaxial loading is under consideration, the nonlinear equation reads (cf. Eq. (69))

$$(1-\phi_1)^2(\bar{T}_1 + 4\bar{T}_2 + \bar{T}_3 + \bar{T}_4 + \bar{T}_5 + 2\bar{T}_6)\bar{\sigma}_{11}^2 = \frac{2}{3}\left\{\sigma_y + h\left[2(1-\phi_1)^2\lambda\sqrt{\frac{2}{3}(\bar{T}_1 + 4\bar{T}_2 + \bar{T}_3 + \bar{T}_4 + \bar{T}_5 + 2\bar{T}_6)}|\bar{\sigma}_{11}|\right]^{\bar{q}}\right\}^2. \tag{71}$$

In the case of a *monotonic* uniaxial loading, the overall uniaxial stress–strain relation can be obtained by integrating Eqs. (68) and (70) as follows:

$$\bar{\boldsymbol{\epsilon}} = \begin{bmatrix} \frac{k_*}{-l_*^2 + k_*\bar{n}_*} & 0 & 0 \\ 0 & \frac{l_*}{2(l_*^2 - k_*\bar{n}_*)} & 0 \\ 0 & 0 & \frac{l_*}{2(l_*^2 - k_*\bar{n}_*)} \end{bmatrix} \bar{\sigma}_{11} + 2(1-\phi_1)^2 \sum_i [(\Delta\lambda)^i(\bar{\sigma}_{11})^i] \times \begin{pmatrix} \bar{T}_1 + 4\bar{T}_2 + \bar{T}_3 + \bar{T}_4 + \bar{T}_5 + 2\bar{T}_6 & 0 & 0 \\ 0 & \bar{T}_3 + \bar{T}_5 & 0 \\ 0 & 0 & \bar{T}_3 + \bar{T}_5 \end{pmatrix}, \tag{72}$$

where $(\Delta\lambda)^i$ is the ith iteration value of $\Delta\lambda$ and $(\bar{\sigma}_{11})^i$ is the i-th iteration value of macroscopic uniaxial stress.

3. Evolutionary interfacial debonding: probabilistic micromechanics

The progressive interfacial debonding may occur under increasing deformations and influence the overall stress–strain behavior of aligned discontinuous fiber-reinforced composites. After the interfacial debonding between fibers and the matrix, the debonded fibers lose the load-carrying capacity in the debonded direction and are regarded as partially debonded fibers. For convenience, following Tohgo and Weng (1994) and Zhao and Weng (1995, 1996, 1997), we employ the average internal stresses of fibers as the controlling factor. The probability of partial debonding is modeled as a two-parameter Weibull process (see Tohgo and Weng (1994), Zhao and Weng (1995), and Ju and Lee (1999)). Assuming that the Weibull (1951) statistics governs, we can express the cumulative probability distribution function of fiber debonding (damage), P_d, at the level of hydrostatic tensile stress as

$$P_d[(\bar{\boldsymbol{\sigma}}_m)_1] = 1 - \exp\left[-\left(\frac{(\bar{\boldsymbol{\sigma}}_m)_1}{S_0}\right)^M\right], \tag{73}$$

where $(\bar{\boldsymbol{\sigma}}_m)_1 = [(\bar{\sigma}_{11})_1 + (\bar{\sigma}_{22})_1 + (\bar{\sigma}_{33})_1]/3$ is the hydrostatic tensile stresses of the fibers, the subscript $(\cdot)_1$ denotes the fiber phase, and S_0 and M are the Weibull parameters.

Therefore, the current partially debonded fiber volume fraction ϕ_2 at a given level of $(\bar{\boldsymbol{\sigma}}_m)_1$ is given by

$$\phi_2 = \phi P_d[(\bar{\boldsymbol{\sigma}}_m)_1] = \phi\left\{1 - \exp\left[-\left(\frac{(\bar{\boldsymbol{\sigma}}_m)_1}{S_0}\right)^M\right]\right\}, \tag{74}$$

where ϕ is the original fiber volume fraction.

The internal stresses of fibers required for the initiation of interfacial debonding were explicitly derived by Ju and Lee (1999). For multi-phase composites, the average internal stresses of fibers can be expressed as

$$\bar{\boldsymbol{\sigma}}_1 = \mathbf{C}_1 \cdot \left[\mathbf{I} - \mathbf{S} \cdot (\mathbf{A}_1 + \mathbf{S})^{-1}\right] \cdot \left[\mathbf{I} - \sum_{m=1}^{2} \phi_m \mathbf{S} \cdot (\mathbf{A}_m + \mathbf{S})^{-1}\right]^{-1} : \bar{\boldsymbol{\epsilon}} \equiv \mathbf{U} : \bar{\boldsymbol{\epsilon}}. \tag{75}$$

By carrying out the lengthy algebra, the components of the positive definite fourth-rank tensor $\mathbf{U}$ are explicitly given by

$$U_{ijkl} = \tilde{F}_{ijkl}(U_1, U_2, U_3, U_4, U_5, U_6), \tag{76}$$

where the definition of fourth-rank tensor $\tilde{\mathbf{F}}$ is given Eq. (8) and the inverse and product of fourth-rank tensor $\tilde{\mathbf{F}}$ are given in the appendix of Ju and Chen (1994b). The components of the fourth-rank tensor $\mathbf{U}$ are given by

$$U_1 = 2\mu_1 \mathscr{D}_1, \tag{77}$$
$$U_2 = 2\mu_1 \mathscr{D}_2, \tag{78}$$
$$U_3 = \lambda_1(\mathscr{D}_1 + 4\mathscr{D}_2 + 3\mathscr{D}_3) + 2\mu_1 \mathscr{D}_3, \tag{79}$$
$$U_4 = 2\mu_1 \mathscr{D}_4, \tag{80}$$
$$U_5 = \lambda_1(\mathscr{D}_4 + 3\mathscr{D}_5 + 2\mathscr{D}_6) + 2\mu_1 \mathscr{D}_5, \tag{81}$$
$$U_6 = 2\mu_1 \mathscr{D}_6, \tag{82}$$

where $\mathscr{D}_1, \ldots, \mathscr{D}_6$ are the parameters of the fourth-rank tensor $\tilde{F}_{ijkl}(\mathscr{D}_1, \ldots, \mathscr{D}_6)$, which is the product between two fourth-rank tensors $\tilde{F}_{ijkl}(j_1, \ldots, j_6)$ and $\tilde{F}_{ijkl}(i_1, \ldots, i_6)$. Parameters $j_1, \ldots, j_6$ are defined as

$$\begin{aligned}
j_1 &= -S_1(b_1 + 4b_2 + b_3 + 2b_6) - 4S_2(b_1 + 2b_2 + b_3) - S_4(b_1 + 4b_2 + 3b_3) - 2S_6 b_1, \\
j_2 &= -2S_2(b_2 + b_6) - 2S_6 b_2, \\
j_3 &= -S_3(b_1 + 4b_2 + b_3 + 2b_6) - S_5(b_1 + 4b_2 + 3b_3) - 2S_6 b_3, \\
j_4 &= -S_1(b_4 + b_5) - 4S_2(b_4 + b_5) - S_4(b_4 + 3b_5 + 2b_6) - 2S_6 b_4, \\
j_5 &= -S_3(b_4 + b_5) - S_5(b_4 + 3b_5 + 2b_6) - 2S_6 b_5, \\
j_6 &= \frac{1}{2} - 2S_6 b_6
\end{aligned} \tag{83}$$

in which the components of Eshelby's tensor for a spheroidal inclusion, $S_1, \ldots, S_6$, are given in Eqs. (20)–(25) and $b_1, \ldots, b_6$ are the parameters of the fourth-rank tensor $\tilde{F}_{ijkl}(b_1, \ldots, b_6)$, which is the inverse of $\tilde{F}_{ijkl}(d_1, \ldots, d_6)$ with the following parameters:

$$\begin{aligned}
&d_1 = S_1, \qquad d_2 = S_2, \qquad d_3 = S_3, \\
&d_4 = S_4, \qquad d_5 = \frac{1}{3}\left(\frac{\kappa_0}{\kappa_1 - \kappa_0} - \frac{\mu_0}{\mu_1 - \mu_0}\right) + S_5, \qquad d_6 = \frac{1}{2}\frac{\mu_0}{\mu_1 - \mu_0} + S_6.
\end{aligned} \tag{84}$$

In addition, $i_1, \ldots, i_6$ are the parameters of the fourth-rank tensor $\tilde{F}_{ijkl}(i_1, \ldots, i_6)$, which is the inverse of $\tilde{F}_{ijkl}(h_1, \ldots, h_6)$ with the following parameters:

$$\begin{aligned}
&h_1 = \phi_1 \bar{c}_1 - \phi_2 g_1, \qquad h_2 = -\phi_1 \bar{c}_2 - \phi_2 g_2, \quad h_3 = -\phi_1 \bar{c}_3 - \phi_2 g_3, \\
&h_4 = -\phi_1 \bar{c}_4 - \phi_2 g_4, \qquad h_5 = -\phi_1 \bar{c}_5 - \phi_2 g_5, \qquad h_6 = \frac{1}{2} - \phi_1 \bar{c}_6 - \phi_2 g_6,
\end{aligned} \tag{85}$$

where $\bar{c}_1, \ldots, \bar{c}_6$ are the parameters of the fourth-rank tensor $\tilde{F}_{ijkl}(\bar{c}_1, \ldots, \bar{c}_6)$, which is the product between two fourth-rank tensors $\tilde{F}_{ijkl}(S_1, \ldots, S_6)$ and $\tilde{F}_{ijkl}(b_1, \ldots, b_6)$. Furthermore, $g_1, \ldots, g_6$ are the parameters of

the fourth-rank tensor $\tilde{F}_{ijkl}(g_1,\ldots,g_6)$, which is the product between two fourth-rank tensors $\tilde{F}_{ijkl}(S_1,\ldots,S_6)$ and $\tilde{F}_{ijkl}(e_1,\ldots,e_6)$. Here, $e_1,\ldots,e_6$ are the parameters of the fourth-rank tensor $\tilde{F}_{ijkl}(e_1,\ldots,e_6)$, which is the inverse of $\tilde{F}_{ijkl}(f_1,\ldots,f_6)$ with the following parameters:

$$f_1 = S_1, \quad f_2 = S_2, \quad f_3 = S_3,$$
$$f_4 = S_4, \quad f_5 = \frac{1}{3}\left(\frac{\kappa_0}{\kappa_2-\kappa_0} - \frac{\mu_0}{\mu_2-\mu_0}\right) + S_5,$$
$$f_6 = \frac{1}{2}\frac{\mu_0}{\mu_2-\mu_0} + S_6. \tag{86}$$

In the case of tensile loading, the averaged internal stresses of fibers can be obtained as follows:

$$(\bar{\sigma}_{11})_1 = (U_1 + 4U_2 + U_3 + U_4 + U_5 + 2U_6)\bar{\epsilon}_{11} + (U_4+U_5)\bar{\epsilon}_{22} + (U_4+U_5)\bar{\epsilon}_{33}, \tag{87}$$
$$(\bar{\sigma}_{22})_1 = (U_3+U_5)\bar{\epsilon}_{11} + (U_5+2U_6)\bar{\epsilon}_{22} + U_5\bar{\epsilon}_{33}, \tag{88}$$
$$(\bar{\sigma}_{33})_1 = (U_3+U_5)\epsilon_{11} + U_5\bar{\epsilon}_{22} + (U_5+2U_6)\bar{\epsilon}_{33}, \tag{89}$$

where $\bar{\epsilon}_{11}$, $\bar{\epsilon}_{22}$ and $\bar{\epsilon}_{33}$ are the total (ensemble-volume averaged) strains in the 1, 2 and 3 directions, respectively.

4. Numerical comparisons and simulations

The numerical and experimental studies to characterize damage evolution in discontinuous fiber-reinforced composites have been limited in the literature until now. One such experimental and numerical study on randomly oriented, discontinuous fiber composites was made by Meraghni and Benzeggagh (1995) and Meraghni et al. (1996). They introduced an experimental damage parameter, β, to allow the modeling of damage mechanisms. A micromechanics-based analytical simulation was also presented and compared with the experimental data.

In order to show the validity of the proposed micromechanical framework, we now compare our analytical predictions with bounds based on Halpin–Tsai micromechanics equations (Halpin and Kardos, 1976). One of the advantages of the Halpin–Tsai equations is that they cover both the particulate-reinforced case (fiber aspect ratio = unity, lower bound) and the continuous fiber case (fiber aspect ratio = infinity, upper bound). Indeed, one can mathematically express the equation limits as the rule of mixtures for continuous fibers and modified Kerner equation for spherical reinforcement. In the case of the upper bound (continuous fiber), the modulus in the fiber direction is given simply by a rule of mixtures

$$E_L = E_{\mathrm{f}}\phi_{\mathrm{f}} + E_{\mathrm{m}}\phi_{\mathrm{m}}, \tag{90}$$

where E_L denotes Young's modulus along the axis of symmetry, and ϕ_{f} and ϕ_{m} are the volume fractions of fiber and the matrix phases, respectively. For particulate filled systems (lower bound), the mathematical theory which is most versatile and best predicts the experimental results over a wide volume fraction range is that due to Kerner (1956). His complete equation is

$$E_L = 2(1+v)\left[\frac{\frac{\phi_1\mu_1}{(7-5v_0)\mu_0+(8-10v_0)\mu_1} + \frac{\phi_0}{15(1-v_0)}}{\frac{\phi_1\mu_0}{(7-5v_0)\mu_0+(8-10v_0)\mu_1} + \frac{\phi_0}{15(1-v_1)}}\right], \tag{91}$$

where subscripts 0 and 1 represent the matrix and filler phases, respectively, and the Poisson ratio, v, is given by

$$v = v_0\phi_0 + v_1\phi_1. \tag{92}$$

For comparisons, the effective Young's modulus along the axis of symmetry for the proposed framework can be obtained as

$$E_L = \bar{n}_* - \frac{l_*^2}{k_*}, \tag{93}$$

where the parameters $\bar{n}_*$, l_* and k_* are given in Eq. (32). We will consider the following constituent elastic properties for carbon fiber polymer matrix composites: $E_0 = 3$ GPa, $v_0 = 0.35$, $E_1 = 380$ GPa and $v_1 = 0.25$. Fig. 2 shows the predicted effective (normalized) Young's moduli in the fiber direction E_L/E_0 of AFPCs at various fiber volume fractions ϕ_1. We plot the theoretical predictions in Fig. 2 based on Halpin–Tsai's bounds and the proposed Eq. (93) with various fiber aspect ratios. Clearly, our analytical predictions are well within the Halpin–Tsai's bounds.

To illustrate the elastoplastic behavior of the present damage constitutive framework, our present damage model considering interfacial debonding is exercised for the case of aligned carbon fiber polymer matrix composites. The material properties used in these simulations are $E_0 = 3.0$ GPa, $v_0 = 0.35$, $E_1 = 380$ GPa, $v_1 = 0.25$, $\sigma_y = 125$ MPa, $h = 400$ MPa and $\bar{q} = 0.5$. In addition, to implement the proposed prob-

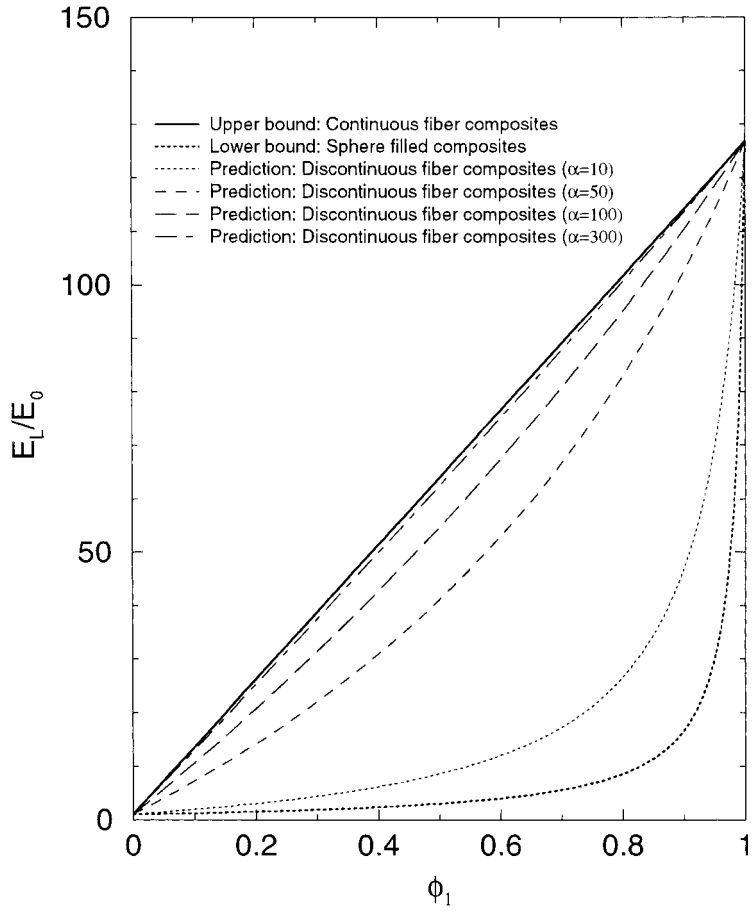

Fig. 2. The comparison between the proposed predictions with various fiber aspect ratios and Halpin–Tsai's bounds for effective Young's modulus in the fiber direction vs. fiber volume fraction.

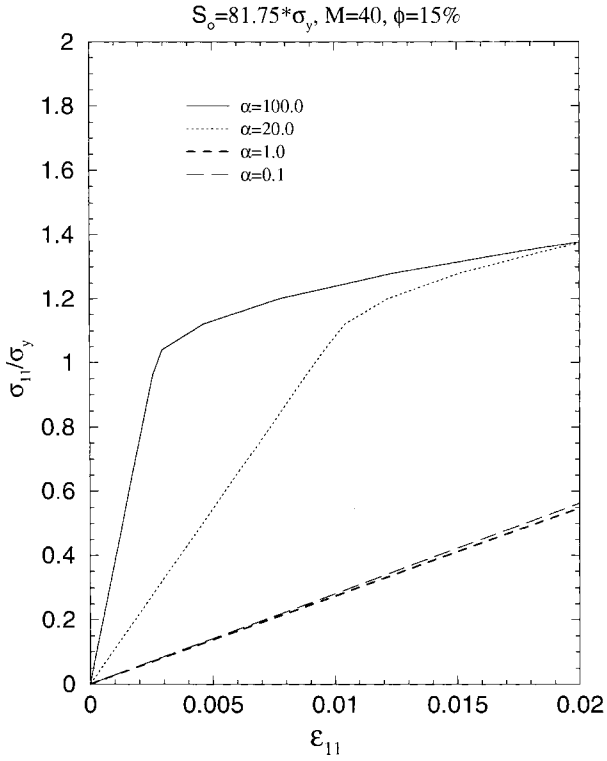

Fig. 3. Effect of the shape of fibers on the overall uniaxial elastoplastic behavior of AFPCs.

abilistic micromechanics based on Weibull function into the present constitutive models, we need to estimate the values of Weibull parameters S_0 and M. For simplicity, we assume the Weibull parameters to be $S_0 = 81.75\sigma_y$ and $M = 40$. Fig. 3 shows the effect of the shape of fibers on the mechanical behavior of AFPCs with the same fiber volume fraction and it clearly shows that the elastoplastic behavior of the composites is strongly dependent on the shape of fibers. Fig. 4 exhibits the effect of the initial fiber volume fraction on the behavior and progressive debonding of the composites and includes the results for perfect composites shown by solid lines and debonded composites shown by dashed lines. Interfacial debonding is not observed for low fiber volume fraction ($\phi = 0.2$) composites. Fig. 5 exhibits the evolution of debonded fiber volume fraction as a function of the uniaxial strain. It is seen that the composite with high initial fiber volume fraction is stiffer, but the influence of damage on the stress–strain response of the composite is more drastic because of quick damage evolution.

5. Conclusion

Based on the ensemble-averaging process and noninteracting effects of eigenstrains due to the existence of discontinuous fibers, a new micromechanical damage constitutive model is presented to predict effective elastoplastic damage behavior of AFPCs. Stress–strain fields outside discontinuous fibers are derived by introducing an unit outnormal vector on the imaginary ellipsoid surface. Progressive interfacial debonding is subsequently considered in accordance with Weibull's probability distribution function to characterize

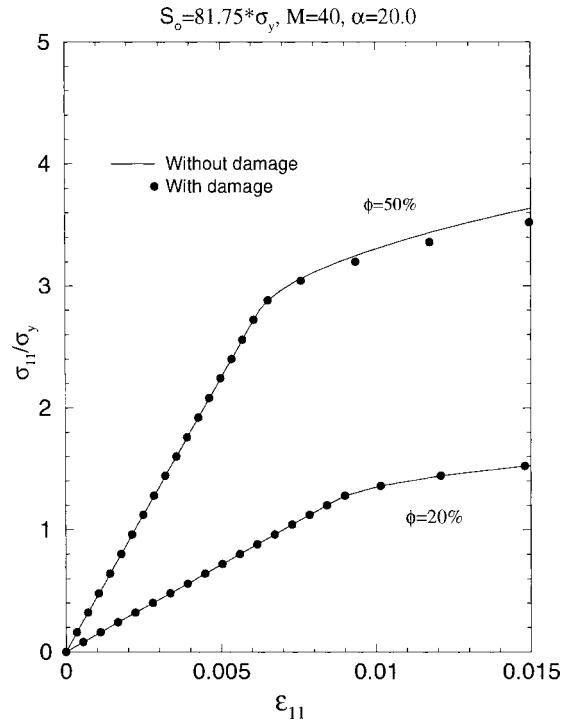

Fig. 4. Effect of the initial volume fraction of fibers on the overall uniaxial elastoplastic behavior and progressive debonding of AFPCs.

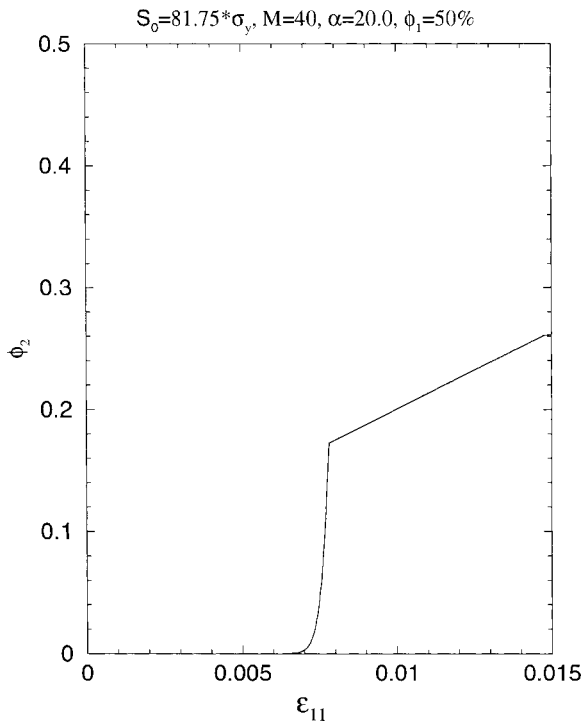

Fig. 5. The predicted evolution of debonded fiber volume fraction corresponding to Fig 4.

the varying probability of fiber debonding. The proposed analytical predictions are compared with Halpin–Tsai's bounds for stiffness predictions. Furthermore, the proposed closed-form damage constitutive model is applied to the uniaxial tensile loading to illustrate damage behavior of AFPCs.

The authors are currently working on the extension of the proposed method to predict the damage behavior of randomly oriented, discontinuous fiber polymer composites (RFPCs). The interaction effect among constituents will be considered in modeling the damage behavior of composites for both moderately and extremely high fiber volume fraction. Other damage mechanisms, such as matrix cracking, void nucleation, etc., will be also included in our damage constitutive models to offer more realistic damage predictions. Finally, the present micromechanical damage constitutive model will be implemented into finite element code to address the progressive crushing in composite structures under impact loading.

Acknowledgements

This research was sponsored by the US Department of Energy, Assistant Secretary for Energy Efficiency and Renewable Energy, Office of Transportation Technologies, Lightweight Materials Program, under the contract DE-AC05-96OR22464 with Lockheed Martin Energy Research Corporation. The research was supported in part by an appointment to the Oak Ridge National Laboratory Postdoctoral Research Associates Program administered jointly by the Oak Ridge National Laboratory and the Oak Ridge Institute for Science and Education.

Appendix A. Parameters $\psi_{11}, \ldots, \psi_{22}$ and $\varphi_1, \ldots, \varphi_3$ in Eq. (31)

These parameters in Eq. (31) take the form

$$\psi_{ij} = \lambda_0 - \sum_{r=1}^{2}\left\{2\mu_0\phi_r\frac{(\eta_r)_{ij}}{(\zeta_r)_i} + \frac{\lambda_0\phi_r}{(\zeta_r)_j} - \lambda_0\phi_r\left[\frac{(\eta_r)_{1j}}{(\zeta_r)_1} + \frac{2(\eta_r)_{2j}}{(\zeta_r)_2}\right]\right\} \quad (i,j=1,2), \tag{A.1}$$

$$\varphi_i = \mu_0\sum_{r=1}^{2}\left[1 + \frac{\phi_r}{(\zeta_r)_i}\right] \quad (i=1,2,3) \tag{A.2}$$

with

$$(\zeta_r)_i = 2[\mathscr{Y}_r + (1-\phi_r)\mathscr{B}_i] \quad (i=1,2,3), \tag{A.3}$$

$$(\eta_r)_{i1} = \frac{(\upsilon_r)_2[\mathscr{X}_r + (1-\phi_r)\bar{\mathscr{A}}_{i1}] - 2(\upsilon_r)_4[\mathscr{X}_r + (1-\phi_r)\bar{\mathscr{A}}_{i2}]}{(\upsilon_r)_1(\upsilon_r)_2 - 2(\upsilon_r)_3(\upsilon_r)_4} \quad (i=1,2,3), \tag{A.4}$$

$$(\eta_r)_{i2} = \frac{(\upsilon_r)_1[\mathscr{X}_r + (1-\phi_r)\bar{\mathscr{A}}_{i2}] - (\upsilon_r)_3[\mathscr{X}_r + (1-\phi_r)\bar{\mathscr{A}}_{i1}]}{(\upsilon_r)_1(\upsilon_r)_2 - 2(\upsilon_r)_3(\upsilon_r)_4} \quad (i=1,2,3), \tag{A.5}$$

and

$$(\upsilon_r)_1 = \mathscr{X}_r + (1-\phi_r)\mathscr{A}_1 + (\zeta_r)_1, \tag{A.6}$$

$$(\upsilon_r)_2 = 2\mathscr{X}_r + 2(1-\phi_r)\mathscr{A}_2 + (\zeta_r)_2, \tag{A.7}$$

$$(\upsilon_r)_3 = \mathscr{X}_r + (1-\phi_r)\mathscr{A}_3, \tag{A.8}$$

$$(\upsilon_r)_4 = \mathscr{X}_r + (1-\phi_r)\mathscr{A}_4 \tag{A.9}$$

in which

$$\mathscr{A}_1 = \bar{\mathscr{A}}_{11},\ \mathscr{A}_2 = \bar{\mathscr{A}}_{22},\ \mathscr{A}_3 = \bar{\mathscr{A}}_{12},\ \mathscr{A}_4 = \bar{\mathscr{A}}_{21}, \tag{A.10}$$

$$\mathscr{B}_1 = \bar{\mathscr{B}}_{11},\ \mathscr{B}_2 = \bar{\mathscr{B}}_{22},\ \mathscr{B}_3 = \bar{\mathscr{B}}_{12}, \tag{A.11}$$

$$\mathscr{X}_r = \frac{\lambda_0\mu_r - \lambda_r\mu_0}{(\mu_r - \mu_0)[2(\mu_r - \mu_0) + 3(\lambda_r - \lambda_0)]}, \tag{A.12}$$

$$\mathscr{Y}_r = \frac{\mu_0}{2(\mu_r - \mu_0)}. \tag{A.13}$$

In addition, the parameters $\bar{\mathscr{A}}_{ij}$ and $\bar{\mathscr{B}}_{ij}$ read

$$\bar{\mathscr{A}}_{11} = \left(4v_0 + \frac{2}{\alpha^2 - 1}\right)\varpi + 4v_0 + \frac{4}{3(\alpha^2 - 1)}, \tag{A.14}$$

$$\bar{\mathscr{A}}_{12} = \bar{\mathscr{A}}_{13} = S_4 + S_5, \tag{A.15}$$

$$\bar{\mathscr{A}}_{21} = \bar{\mathscr{A}}_{31} = S_3 + S_5, \tag{A.16}$$

$$\bar{\mathscr{A}}_{22} = \bar{\mathscr{A}}_{23} = \bar{\mathscr{A}}_{32} = \bar{\mathscr{A}}_{33} = S_5, \tag{A.17}$$

$$\bar{\mathscr{B}}_{11} = \left(-4v_0 + \frac{4\alpha^2 - 2}{\alpha^2 - 1}\right)\varpi - 4v_0 + \frac{12\alpha^2 - 8}{3(\alpha^2 - 1)}, \tag{A.18}$$

$$\bar{\mathscr{B}}_{12} = \bar{\mathscr{B}}_{21} = \bar{\mathscr{B}}_{13} = \bar{\mathscr{B}}_{31} = S_2 + S_6, \tag{A.19}$$

$$\bar{\mathscr{B}}_{22} = \bar{\mathscr{B}}_{33} = \bar{\mathscr{B}}_{23} = \bar{\mathscr{B}}_{32} = S_6, \tag{A.20}$$

where the components of Eshelby's tensor $S_1, \ldots, S_6$ and ϖ are given in Eqs. (20)–(25) and (26), respectively.

Appendix B. Parameters $\mathscr{M}_{ij}$ and $\mathscr{N}_i$ in Eq. (42)

These parameters are given by

$$\begin{aligned}\mathscr{M}_{ij} = & -\frac{1}{3} + \sum_{r=1}^{2} \frac{2\phi_r}{4725(1 - v_0)^2(\mathscr{V}_r)_i(\mathscr{V}_r)_j}\{1575(1 - 2v_0)^2(\mathscr{W}_r)_{ii}(\mathscr{W}_r)_{jj} \\ & + 21(25v_0 - 23)(1 - 2v_0)[(\mathscr{W}_r)_{ii}\mathscr{U}_j + (\mathscr{W}_r)_{jj}\mathscr{U}_i] \\ & + 21(25v_0 - 2)(1 - 2v_0)[(\mathscr{W}_r)_{ii} + (\mathscr{W}_r)_{jj}] + 3(35v_0^2 - 70v_0 + 36)\bar{\mathscr{U}}_{ij} \\ & + 7(50v_0^2 - 59v_0 + 8)(\mathscr{U}_i + \mathscr{U}_j) - 2(175v_0^2 - 343v_0 + 103)\} \quad (i, j = 1, 2),\end{aligned} \tag{B.1}$$

$$\begin{aligned}\mathscr{N}_i = & \frac{1}{2} + \sum_{r=1}^{2} \frac{\phi_r}{1575(1 - v_0)(\mathscr{V}_r)_i(\mathscr{V}_r)_i}\left\{(72 - 140v_0 + 70v_0^2)\mathscr{Q}_i - (75 - 266v_0 + 175v_0^2)\frac{\mathscr{R}_i}{2}\right. \\ & \left. + (164 - 476v_0 + 350v_0^2)\right\} \quad (i = 1, 2, 3),\end{aligned} \tag{B.2}$$

where

$$\mathscr{Q}_1 = b, \quad \mathscr{Q}_2 = d, \quad \mathscr{Q}_3 = c, \tag{B.3}$$

$$\mathscr{R}_1 = \mathscr{Q}_1 + \mathscr{Q}_2, \quad \mathscr{R}_2 = 2\mathscr{Q}_2, \quad \mathscr{R}_3 = \mathscr{Q}_1 + \mathscr{Q}_2, \tag{B.4}$$

$$(\mathscr{V}_r)_i = 2(\mathscr{Y}_r + \mathscr{B}_i) \quad (i = 1,2,3), \tag{B.5}$$

$$(\mathscr{W}_r)_{i1} = \frac{(Z_r)_{i1}}{J_r} \quad (i = 1,2,3), \tag{B.6}$$

$$(\mathscr{W}_r)_{i2} = (\mathscr{W}_r)_{i3} = \frac{(Z_r)_{i2}}{J_r} \quad (i = 1,2,3) \tag{B.7}$$

in which $\mathscr{Y}_r$ and $\mathscr{B}_i$ are given in Eqs. (A.13) and (A.12), respectively, and

$$(Z_r)_{i1} = [2\mathscr{X}_r + 2\mathscr{A}_2 + (\mathscr{V}_r)_2][\mathscr{X}_r + \bar{\mathscr{A}}_{i1}] - 2[\mathscr{X}_r + \mathscr{A}_3][\mathscr{X}_r + \bar{\mathscr{A}}_{i2}] \quad (i = 1,2,3), \tag{B.8}$$

$$J_r = [2\mathscr{X}_r + 2\mathscr{A}_2 + (\mathscr{V}_r)_2][\mathscr{X}_r + \mathscr{A}_1 + (\mathscr{V}_r)_1] - 2[\mathscr{X}_r + \mathscr{A}_3][\mathscr{X}_r + \mathscr{A}_4], \tag{B.9}$$

$$(Z_r)_{i2} = [2\mathscr{X}_r + \mathscr{A}_1 + (\mathscr{V}_r)_1][\mathscr{X}_r + \bar{\mathscr{A}}_{i2}] - [\mathscr{X}_r + \mathscr{A}_3][\mathscr{X}_r + \bar{\mathscr{A}}_{i1}] \quad (i = 1,2,3). \tag{B.10}$$

In addition, the components of $\mathscr{U}_i$ and $\bar{\mathscr{U}}_{ij}$ in Eq. (B.1) read

$$\mathscr{U}_1 = \frac{3[1 - \alpha^4 f(\alpha^2)]}{1 - \alpha^4}, \tag{B.11}$$

$$\mathscr{U}_2 = \mathscr{U}_3 = \tfrac{1}{2}(3 - \mathscr{U}_1), \tag{B.12}$$

$$\bar{\mathscr{U}}_{ij} = \begin{bmatrix} b & c & c \\ c & d & d \\ c & d & d \end{bmatrix} \quad (i,j = 1,2,3) \tag{B.13}$$

with

$$f(\alpha) = \begin{cases} \frac{\cos^{-1}\alpha}{\alpha\sqrt{1-\alpha^2}}, & \alpha < 1, \\ \frac{\cosh^{-1}\alpha}{\alpha\sqrt{\alpha^2-1}}, & \alpha > 1, \end{cases} \tag{B.14}$$

and

$$b = \frac{5}{2(1-\alpha^4)^2}[2 + \alpha^4 - 3\alpha^4 f(\alpha^2)], \tag{B.15}$$

$$c = \frac{15\alpha^4}{4(1-\alpha^4)^2}[-3 + (1 + 2\alpha^4) f(\alpha^2)], \tag{B.16}$$

$$d = \tfrac{1}{8}(15 - 3b - 4c). \tag{B.17}$$

Appendix C. Components $\bar{T}_1, \ldots, \bar{T}_6$ in Eq. (59)

These components are given by

$$\begin{aligned}
\bar{T}_1 &= 4p_1p_6\bar{t}_6 + 8(p_1+2p_2+p_3)(p_2\bar{t}_2 + p_6\bar{t}_2 + p_2\bar{t}_6) + (p_1+4p_2+3p_3)\\
&\quad\times(p_1\bar{t}_4 + 4p_2\bar{t}_4 + p_4\bar{t}_4 + 2p_6\bar{t}_4 + p_1\bar{t}_5 + 4p_2\bar{t}_5 + 3p_4\bar{t}_5 + 2p_4\bar{t}_6)\\
&\quad+(p_1+4p_2+p_3+2p_6)[2p_6\bar{t}_1 + 4p_2(\bar{t}_1+2\bar{t}_2+\bar{t}_3) + p_4(\bar{t}_1+4\bar{t}_2+3\bar{t}_3)\\
&\quad\quad+p_1(\bar{t}_1+4\bar{t}_2+\bar{t}_3+2\bar{t}_6)], \qquad (C.1)\\
\bar{T}_2 &= 4(p_2p_2\bar{t}_2 + 2p_2p_6\bar{t}_2 + p_6p_6\bar{t}_2 + p_2p_2\bar{t}_6 + 2p_2p_6\bar{t}_6), \qquad (C.2)\\
\bar{T}_3 &= 4p_3p_6\bar{t}_6 + (p_1+4p_2+3p_3)(p_3\bar{t}_4 + p_5\bar{t}_4 + p_3\bar{t}_5 + 3p_5\bar{t}_5 + 2p_6\bar{t}_5 + 2p_5\bar{t}_6)\\
&\quad+(p_1+4p_2+p_3+2p_6)[2p_6\bar{t}_3 + p_5(\bar{t}_1+4\bar{t}_2+3\bar{t}_3) + p_3(\bar{t}_1+4\bar{t}_2+\bar{t}_3+2\bar{t}_6)], \qquad (C.3)\\
\bar{T}_4 &= 4p_4p_6\bar{t}_6 + 8(p_4+p_5)(p_2\bar{t}_2 + p_6\bar{t}_2 + p_2\bar{t}_6) + (p_4+3p_5+2p_6)\\
&\quad\times(p_1\bar{t}_4 + 4p_2\bar{t}_4 + p_4\bar{t}_4 + 2p_6\bar{t}_4 + p_1\bar{t}_5 + 4p_2\bar{t}_5 + 3p_4\bar{t}_5 + 2p_4\bar{t}_6) + (p_4+p_5)\\
&\quad\times[2p_6\bar{t}_1 + 4p_2(\bar{t}_1+2\bar{t}_2+\bar{t}_3) + p_4(\bar{t}_1+4\bar{t}_2+3\bar{t}_3) + p_1(\bar{t}_1+4\bar{t}_2+\bar{t}_3+2\bar{t}_6)], \qquad (C.4)\\
\bar{T}_5 &= 4p_5p_6\bar{t}_6 + (p_4+3p_5+2p_6)(p_3\bar{t}_4 + p_5\bar{t}_4 + p_3\bar{t}_5 + 3p_5\bar{t}_5 + 2p_6\bar{t}_5 + 2p_5\bar{t}_6)\\
&\quad+(p_4+p_5)[2p_6\bar{t}_3 + p_5(\bar{t}_1+4\bar{t}_2+3\bar{t}_3) + p_3(\bar{t}_1+4\bar{t}_2+\bar{t}_3+2\bar{t}_6)], \qquad (C.5)\\
\bar{T}_6 &= 4p_6p_6\bar{t}_6. \qquad (C.6)
\end{aligned}$$

References

Caslini, M., Zanotti, C., O'Brien, T.K., 1987. Study of matrix cracking and delamination in glass/epoxy laminates. J. Compos. Technol. Res. 9, 121–130.

Eshelby, J.D., 1957. The determination of the elastic field of an ellipsoidal inclusion, and related problems. Proc. R. Soc. Lond. A 241, 376–396.

Eshelby, J.D., 1959. The elastic field outside an ellipsoidal inclusion. Proc. R. Soc. Lond. A 252, 561–569.

Eshelby, J.D., 1961. Elastic inclusions and inhomogeneities. In: Progress in Solid Mechanics, vol. II. North-Holland, Amsterdam, pp. 87–140.

Goodier, J.N., 1937. On the integration of the thermo-elastic equations. Phil. Mag. 23, 1017–1032.

Groves, S.E., Harris, C.E., Highsmith, A.L., Allen, D.H., Norvell, R.G., 1987. An experimental and analytical treatment of matrix cracking in cross-ply laminates. Exp. Mech., 73–79.

Halpin, J.C., Kardos, J.L., 1976. The Halpin–Tsai equations: A review. Polym. Engng. Sci. 16, 344–352.

Hill, R., 1964. Theory of mechanical properties of fiber-strengthened materials: I. Elastic behavior. J. Mech. Phys. Solids 12, 199–212.

Ju, J.W., Chen, T.M., 1994a. Micromechanics and effective moduli of elastic composites containing randomly dispersed ellipsoidal inhomogeneities. Acta Mech. 103, 103–121.

Ju, J.W., Chen, T.M., 1994b. Effective elastic moduli of two-phase composites containing randomly dispersed spherical inhomogeneities. Acta Mech. 103, 123–144.

Ju, J.W., Lee, H.K., 1999. A micromechanical damage model for effective elastoplastic behavior of ductile matrix composites considering evolutionary complete particle debonding. J. Comput. Meth. Appl. Mech. Engng., in press.

Ju, J.W., Sun, L.Z., 1998. A novel formulation for the exterior-point Eshelby's tensor of an ellipsoidal inclusion. J. Appl. Mech., submitted for publication.

Kerner, E.H., 1956. The elastic and thermo-elastic properties of composite media. Proc. Phys. Soc. 69 B, 808–813.

Krajcinovic, D., 1996. Damage Mechanics, Series title: North-Holland series in applied mathematics and mechanics, vol. 14. Elsevier, Amsterdam.

Kutlu, Z., Chang, F.K., 1995. Composite panels containing multiple through-the-width delaminations and subjected to compression. Part I: Analysis. Compos. Struct. 31, 273–296.

Matzenmiller, A., Schweizerhof, K., 1991. Crashworthiness simulations of composite structures – a first step with explicit time integration. CAD-FEM GmbH, Munchen.

Meraghni, F., Benzeggagh, M.L., 1995. Micromechanical modeling of matrix degradation in randomly discontinuous-fibre composites. Compos. Sci. Technol. 55, 171–186.

Meraghni, F., Blakeman, C.J., Benzeggagh, M.L., 1996. Effect of interfacial decohesion on stiffness reduction in a random discontinuous-fibre composite containing matrix microcracks. Compos. Sci. Technol. 56, 541–555.

Mura, T., 1987. Micromechanics of Defects in Solids, second ed.. Martinus Nijhoff, The Netherlands.

Mura, T., Shodja, H.M., Hirose, Y., 1996. Inclusion problems. Appl. Mech. Rev. 49, S118–S127.

Nemat-Nasser, S., Hori, M., 1993. Micromechanics: Overall Properties of Heterogeneous Materials. North-Holland, Amsterdam.

Sun, L.Z., 1998. Micromechanics and overall elastoplasticity of discontinuously reinforced metal matrix composites. Ph.D. Dissertation, University of California, Los Angeles.

Tohgo, K., Weng, G.J., 1994. A progress damage mechanics in particle-reinforced metal–matrix composites under high triaxial tension. J. Eng. Mat. Tech. 116, 414–420.

Wang, A.S.D., 1984. Fracture mechanics of sublaminate cracks in composite materials. Compos. Technol. 6, 45–62.

Weibull, W., 1951. A statistical distribution function of wide applicability. J. Appl. Mech. 18, 293–297.

Zhao, Y.H., Weng, G.J., 1995. A theory of inclusion debonding and its influence on the stress–strain relations of a ductile matrix. Int. J. Dam. Mech. 4, 196–211.

Zhao, Y.H., Weng, G.J., 1996. Plasticity of a two-phase composite with partially debonded inclusions. Int. J. Plasticity 12 (6), 781–804.

Zhao, Y.H., Weng, G.J., 1997. Transversely isotropic moduli of two partially debonded composites. Int. J. Solids Struct. 34 (4), 493–507.